

解説

Surface Passivation investigations by Synchrotron Radiation Photoelectron Spectroscopy and the X-Ray Standing Wave Technique

T. Scimeca, M. Oshima and Y. Naninch*

NTT Interdisciplinary Research Laboratories

*Institute of Materials Science, University of Tsukuba

1. Introduction

The development of compound semiconductor based electronic devices (especially GaAs) has been impeded by a high number of surface states that pin the Fermi level near midgap. In 1980, Massies et al.¹⁾ were the first to use sulfur as a way of treating the GaAs surface. However, it was not until 1987 that Sandroff et al.²⁾ reported dramatically improved heterojunction bipolar transistor (HBT) gains as a result of treating the GaAs surface with an aqueous sulfur solution. These gains were widely interpreted as direct evidence that treating the surface with sulfur resulted in a drastic decrease in the number of defects at the GaAs surface. The work also ignited a flurry of activity with electrical characteristic measurements³⁾⁻¹²⁾ (Photoluminescence, C-V and I-V) all indicating a drastic reduction in surface defects following treatment of the GaAs surface with sulfur. While there is debate over whether the Fermi level is unpinned, DLTS measurements indicate that the GaAs midgap state is virtually removed with only one defect state remaining near the valence bands¹³⁾. Since midgap states are most efficient as recombination centers¹⁴⁾, the results show that even if the Fermi level remains pinned, an improved surface results in fewer defect states that can act as recombination traps. A typical example of the improved quality for three

III-V compound semiconductor surfaces is shown in **Fig.1**⁵⁾. Here, the Schottky Barrier Height (SBH) is plotted for the deposition of three different metals (In, Al and Au) on three different III-V compound semiconductors. The results clearly demonstrate that the SBH exhibits a greater dependence on the work function of the deposited metal for the cases where the surface was treated with Sulfur. While the SBH values for the S treated cases are not what one expects in the ideal case where the Fermi level is completely unpinned, the improvement with respect to the as etched GaAs surfaces is significant. Several years after the initial flurry of work on sulfur passivation, Sandroff and others reported the effectiveness of Se in passivating the GaAs surface¹⁵⁻¹⁹⁾. While both S and Se are group VI elements, Se is advantageous in that the diameter of Se is similar to Ga and As and is ultra high vacuum compatible. In contrast, S forms more stable compounds. Details of the structure and chemical bonding of the S and Se treated GaAs surface under a variety of conditions will be discussed later in more detail.

The diagram in **Fig.2** is shown to illustrate the diversity and relevance of surface passivation. The goal of this work is to fabricate high quality surfaces and interfaces that are necessary for manufacturing special electronic devices. Progress has been limited

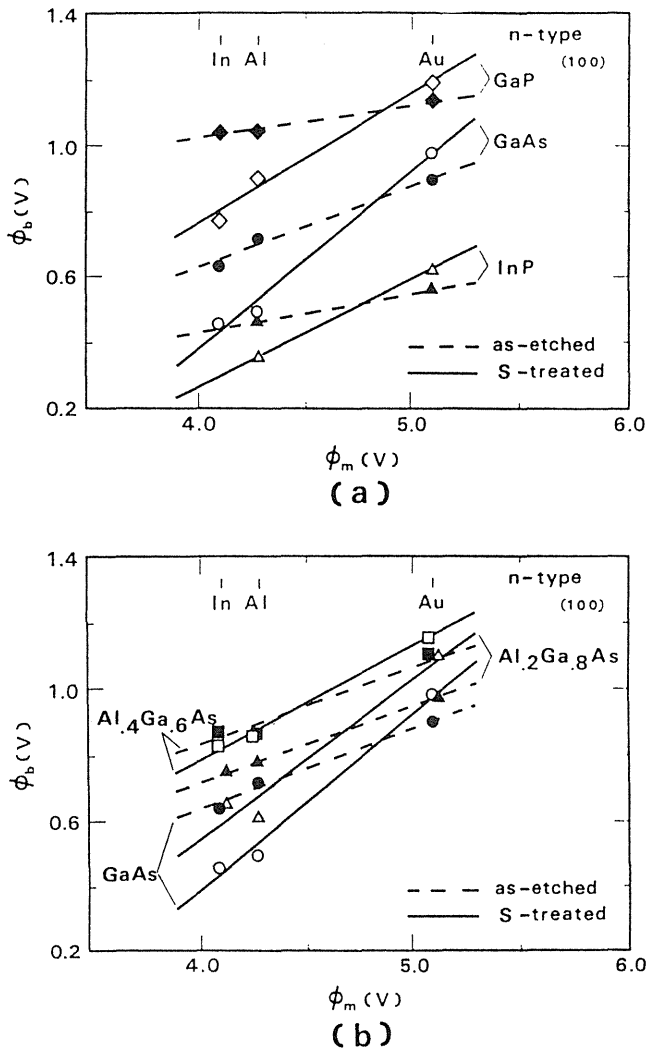


Fig.1 The Schottky Barrier Height(SBH) is plotted for In, Al and Au deposited on GaP, GaAs and InP for the as treated and S treated III-V semiconductor surface.

due to the high number of surface defect states. In addition to GaAs, InP and GaP are also promising materials that have also been the subject of surface passivation studies²⁰⁾⁻²⁸⁾ since surface defects are unacceptably large for these materials. By examining different means of surface passivation by S and Se in a variety of forms and techniques²⁹⁾⁻³³⁾, greater insight into surface passivation and more effective surface passivation methods may be found. Additional investigations into surface passivation by changing the overlayer and the possibility of using materials other than S and Se for passivation are also possible. Finally, it should be stated that a wide variety of

devices ranging from lasers to transistors and even solar cells have benefitted from dramatically improved properties resulting from surface passivation³⁴⁾⁻³⁹⁾. Because of space and time limitations, the work reported here will focus on surface studies relating to the passivation of GaAs surface by S and Se. In addition, the Al/S/GaAs, CaF₂/S/GaAs and Pd/S/GaAs systems will also be discussed illustrating a number of distinct processes that take place at these interfaces. Finally surface segregation and oxidation, which remain two serious problems associated with surface passivation, will be considered.

2. Experimental

The Photoelectron and X-Ray Standing Wave experiments were both performed on Beamline 1A at the Photon Factory in Tsukuba. A schematic of the instrument used in the photoelectron measurements is shown in Fig.3⁴⁰⁾. In this surface analysis system, one of the key characteristics is that an MBE chamber is connected to the analysis chamber. Thus, one can prepare surface and interfaces in a very controlled way in the MBE chamber and transfer them without breaking vacuum to the surface analysis system where the SRPES measurements are carried out. In addition, the surface structure can be monitored both by Reflection High Energy Electron Diffraction(RHEED) and/or Low Energy Electron Diffraction (LEED). In the photoelectron experiments, the synchrotron photon energy was adjusted using a grating/crystal monochromator⁴¹⁾ to obtain surface sensitive information for the synchrotron radiation photoelectron spectroscopy (SRPES) measurements. An excitation energy of 210 eV was used for the S treated samples, thus allowing one to effectively excite the S 2p electrons. A photon energy near 90 eV was used for the Se treated GaAs systems. The total energy resolution is near 0.3 and 0.5 eV for 90 and 210 eV excitation respectively.

As an aid in the interpretation of the photoelectron results to be presented shortly, an energy level diagram for an n type semiconductor is shown in Fig.4. The solid line represents a typical case where there is a significant degree of band bending as a

Substrate	Passivation Agent	Parameters
GaAs, InP, GaP	Sulfur Selenium Tellurium Silicon	Temperature Laser, Elec. Irrad. Method (Dip, MBE, Electrodep.) Crystal Orientation
	Buffer Insulator/Se VDW Solids	

Fabricate good surfaces and interfaces

Devices:
Metal-Semiconductors with High Schottky Barrier Height

M-I-S Structures with low Interface DOS

Heterojunctions

Solar Cells

Fig.2 A diagram illustrating the rich variety of surface passivation studies possible that may lead to the fabrication of high quality surfaces and interfaces and ultimately high performance electronic devices.

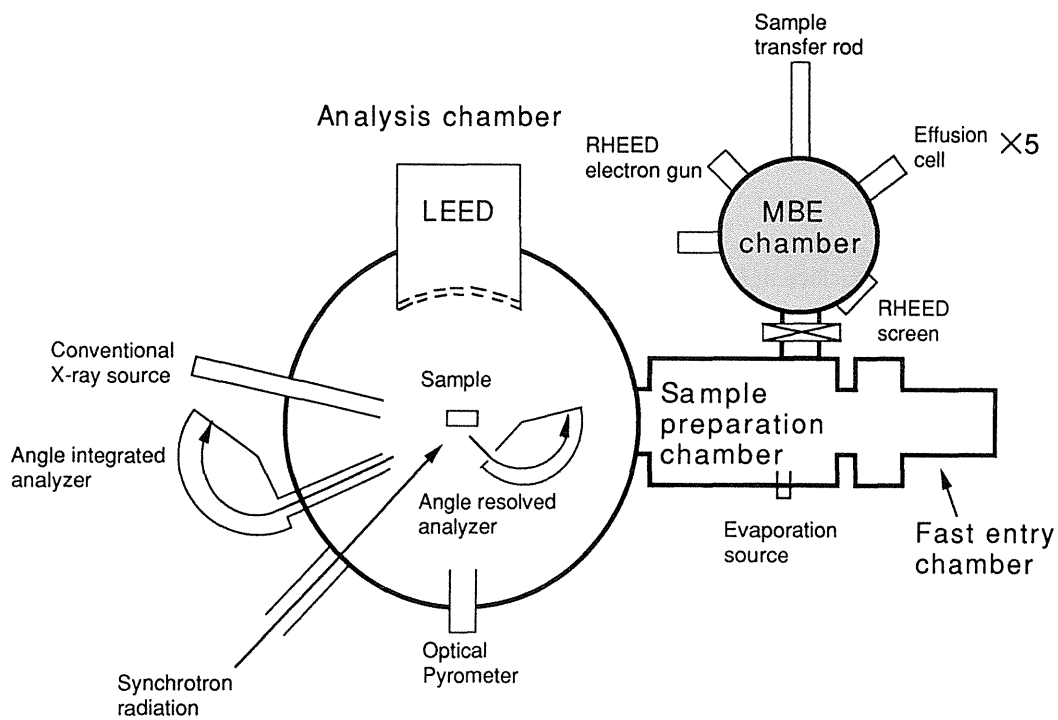
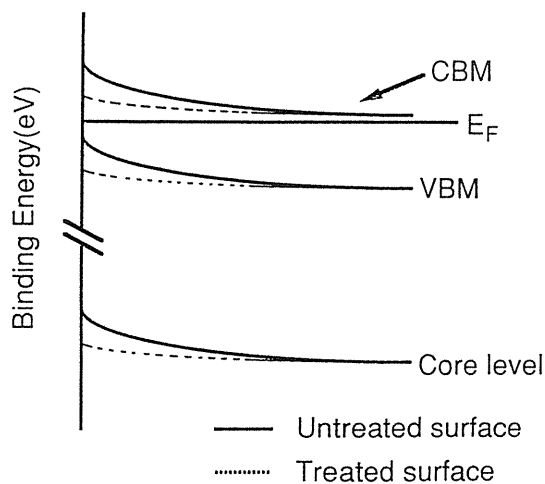


Fig.3 A schematic diagram of the instrument used in the Synchrotron Radiation Photoelectron spectroscopy(SRPES) measurements.

Band bending and photoelectron spectral shifts



Band bending for n type:
Band flattening \rightarrow Increasing Binding Energy

Fig.4 A schematic diagram illustrating band bending in the depletion region for an n type semiconductor. The treated surface corresponds to a reduction in surface defect states and a concomitant relaxation in band bending. The degree of band bending is identical for valence and core levels and is easily probed by energy shifts observed in photoelectron spectroscopy.

result of a high number of surface defect states. As a result of surface passivation, the surface defect density of states is reduced which in turn relaxes band bending in the depletion region. A relaxation in band bending can be observed as a shift towards increasing binding energy either in the valence band maximum (VBM) or core levels in the semiconductor. In this way, Photoelectron Spectroscopy provides a valuable means of correlating the density of surface defect states and surface chemical bonding changes.

A schematic of the instrument used in the x-ray standing wave (XSW) measurement is shown in Fig.5⁴²⁾. An incident beam of 3.1 keV obtained from a double crystal InSb (111) monochromator was used to generate the X-Ray Standing Wave with the emission data collected by scanning around the GaAs(111) Bragg diffraction angle. The special characteristics of this instrument include precise angle scanning in UHV and analysis of light elements

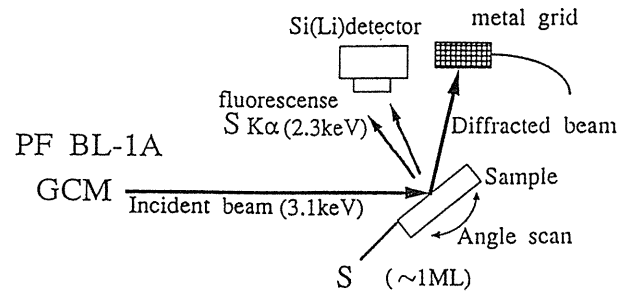


Fig.5 A schematic diagram of the instrument used in the X-Ray Standing Wave(XSW) measurements.

such as Al, Si, P, and S since soft x-rays are used as the excitation source. The diffracted beam was measured directly by a metal grid while the fluorescence intensity was measured by a Si (Li) detector. Owing to the relatively large escape depth of x-rays, one has the capability of analyzing buried interfaces with thick overlayers in a nondestructive manner. The instruments used for the SRPES and XSW measurements are described in detail elsewhere⁴⁰⁾⁻⁴²⁾.

In contrast to photoelectron spectroscopy where the basic principles are well known by a wide range of people, the XSW technique still merits some introduction⁴³⁾. The basic principle of the XSW technique is illustrated in Fig.6. In this figure, the region in which the standing wave is generated is shown in the top of this figure. By varying the substrate angle, the position of the standing wave with respect to the crystal planes can be varied. This is shown on the left bottom side of this figure. Thus, if the position of the designated atom coincides with a nodal point, the standing wave will not excite the atom resulting in little or no generation of photoelectrons or fluorescence x-rays from the designated atom. In contrast the reverse is expected when the x-ray standing wave antinodal point coincides with the position of the designated atom. Thus, by varying the sample angle; the position of the designated atom can be precisely determined with respect to the crystal planes. In addition, the degree of positional disorder can also be determined by analysis of the broadening in the XSW profile. As expected, a broadening of the distribution

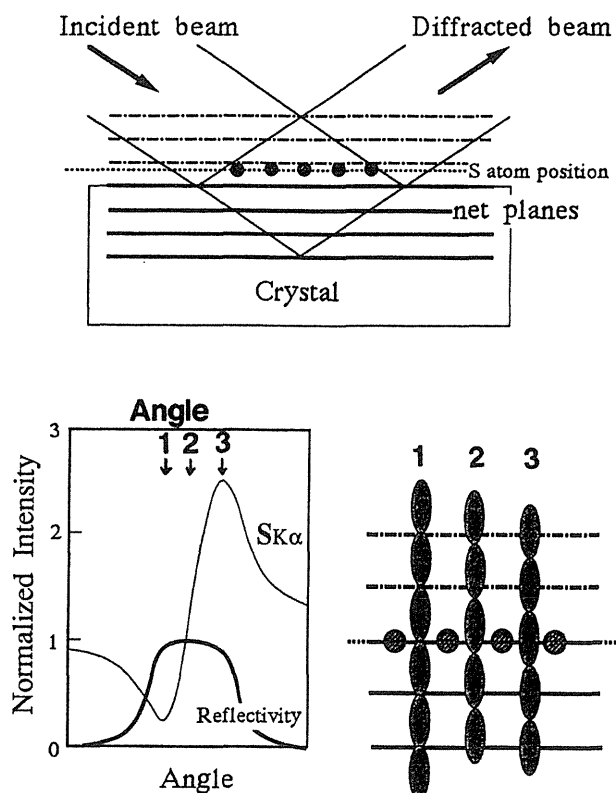


Fig.6 A diagram illustrating the general principles of the XSW technique.

of atomic positions yields a broadening in the XSW generated yield of the designated atom. The intensity of the XSW generated signal (fluorescence or photoelectron signal) can be expressed by the following equation:

$$Y(\theta) = 1 + R(\theta) + 2CF(R(\theta))^{1/2} \cos(2\pi P - \delta(\theta)) \quad (1.1)$$

where $R(\theta)$ is the Drawin-Prins reflectivity of the crystal, δ is the phase shift between the standing x-ray wave and the incident x-ray wave, F is the structural factor, and C is the polarization factor. Two additional parameters in the XSW equation are P , the average atomic position of the designated atom, and F which is related to the distribution of the designated atoms around this average position. This will be understood more clearly as we move on to specific studies. In this paper, the XSW results concentrate on the sulfur treated GaAs(111)A and (111)B surfaces. The reason for excluding the (100) surface is that

Bragg Diffraction on the (100) surface is very small owing to the nearly low Structure Factor(F) for this crystal face. Difficulties with resolving the Se L fluorescence peak from the Ga L and As L peaks prevent analysis of Se treated GaAs substrates by fluorescence detection XSW.

The samples were n type GaAs wafers(Si doped). Sulfur passivation was achieved by first immersing the GaAs wafer in a $(\text{NH}_4)_2\text{S}_x$ solution at 60°C for 1 hour. The Ammonium Sulfide solution is particularly effective in passivating the GaAs surface because the basicity of this solution etches the GaAs leaving a pristine surface upon which the excess sulfur(x is normally 3) adsorbs on⁴⁰. The wafer was then placed in vacuum where the residual amorphous S over-layers sublimes leaving only a monolayer or so of sulfur. A schematic of the surface preparation is shown in Fig.7. Deposition of the Al, CaF_2 and Pd overlayers were done in-situ, but with the substrate at room temperature. Se passivation was achieved by first chemically cleaning the wafer in acetone, deionized water and a commercial alkali etchant. The wafer was then annealed under an As atmosphere until the surface oxides were removed. Following this, Se was deposited under a variety of substrate temperatures.

3. Surface Passivation

A. Sulfur

As mentioned earlier, sulfur surface passivation has been shown to improve the overall electrical characteristics of GaAs. Inquiries into the mechanism responsible for the improved properties of the S treated GaAs surface resulted in numerous surface studies⁴⁵⁻⁵⁵. Initially, the passivation effect was attributed to S bonding to As⁴⁵⁻⁵⁰. However, soon studies began to indicate that while S predominately to As during treatment, the full effects of passivation are not realized until a S-As to S-Ga exchange reaction, most commonly induced by annealing in vacuum, takes places⁵¹⁻⁵⁵. A typical example of the temperature dependence on the chemical bonding of the surface is illustrated by Fig.8, which is a plot of the S 2p spectra for the S/GaAs(111)B surface as a

function of substrate temperature. In this experiment, the substrate temperature was increased at a rate of 10 °C /min. while the S 2p spectra were recorded. Prior to annealing (RT), the S 2p spectrum indicates S bonding to both As and Ga. However, at a substrate temperature near 200 °C , an As-S to Ga-S exchange reaction takes place that is consistent with the greater thermodynamic stability of the Ga-S bond⁵⁶. This exchange reaction is also accompanied by a reduction in the number of surface defects states⁵¹⁻⁵⁵. At this stage, the surface becomes well ordered and a 1 × 1 LEED structure is observed. Prior to S desorption, two S pre-desorption states are observed for the (111)B surface. The nature of these states is not well understood at present, but a similar phenomenon is also observed for the (111)A surface. The S desorp-

tion temperature was also found to correlate with crystal orientation and is discussed in detail elsewhere⁵⁵.

To investigate this study further, a photoluminescence(PL) measurement was performed in-situ in order to correlate the surface chemical bonding changes with surface defect density changes⁵⁷. In photoluminescence, a higher number of defects can act as recombination centers for the generated electron-hole pair, thus reducing the PL intensity. Therefore, a greater PL intensity indicates a reduction in defect states. In **Fig.9**, the PL intensity is plotted as a function of annealing temperature for the sulfur

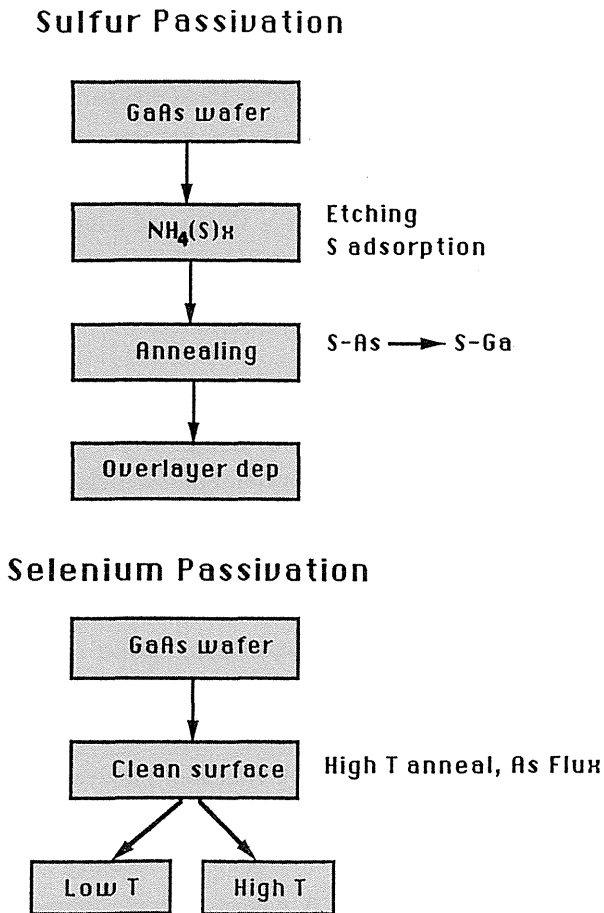


Fig.7 The sequence of events in surface preparation are outlined in this figure.

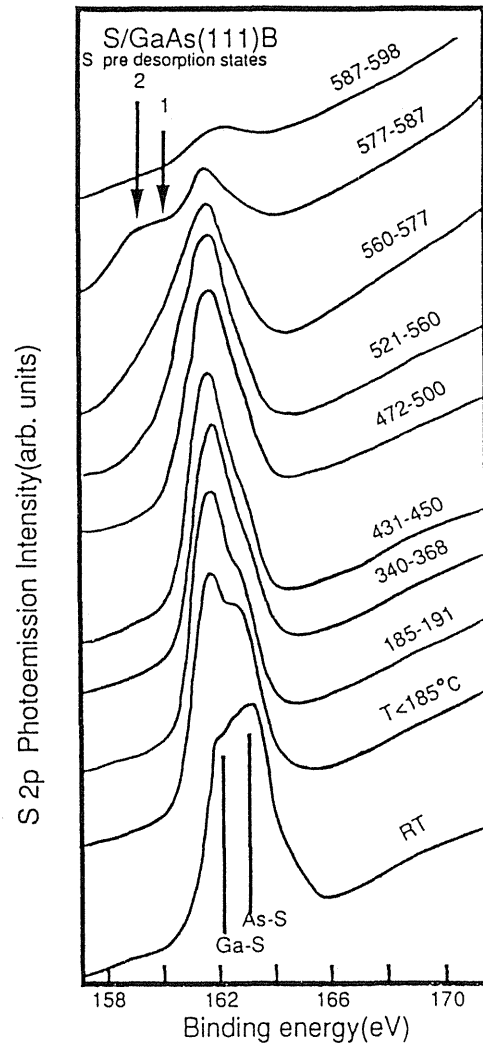


Fig.8 The S 2p spectra are plotted as a function of annealing temperature for the S/GaAs(111)B surface.

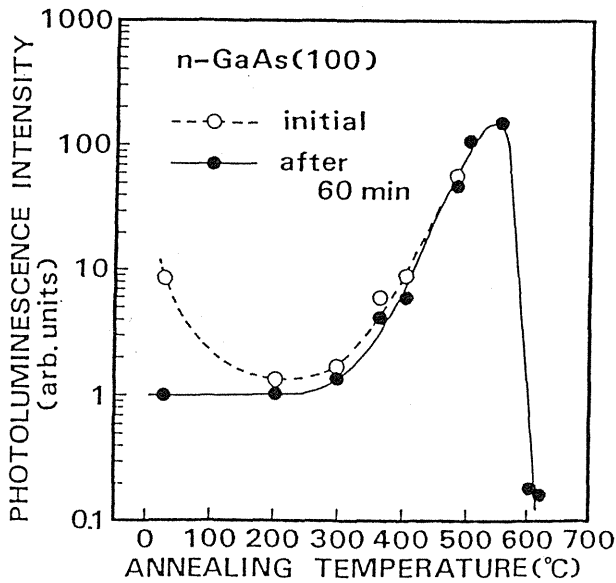


Fig.9 The photoluminescence(PL) intensity is recorded as a function of annealing temperature for the sulfur treated GaAs(100).

treated GaAs(100) surface. The results indicate that annealing at relatively high temperatures is necessary to realize the full effects of surface passivation. This correlates well with the As-S to Ga-S exchange reaction shown in Fig.8. In the neighborhood of 600 °C, S is desorbed from the surface resulting in a Ga rich surface with many defect states and a drastic reduction in the PL intensity.

The As-S to Ga-S exchange reaction is not only thermodynamically reasonable⁵⁶⁾, but also results in a lower density of states in the band gap of GaAs^{58), 59)} and is also consistent with the Advanced Unified Defect model⁶⁰⁾ and Disordered Induced Gap States(DIGS) model⁶¹⁾.

The next figure(Fig.10) is a plot of the S 2p spectra for three different crystal orientation of GaAs. There are two main differences between the top set of curves where the GaAs substrate was annealed at 480 °C for 10 min and the bottom set of spectra where the GaAs samples were not annealed. The first difference lies in the main region of the S 2p spectra (160-166eV) where the non annealed samples exhibit a range of As-S and Ga-S bonding that is more likely a result of prior sample treatment. However upon

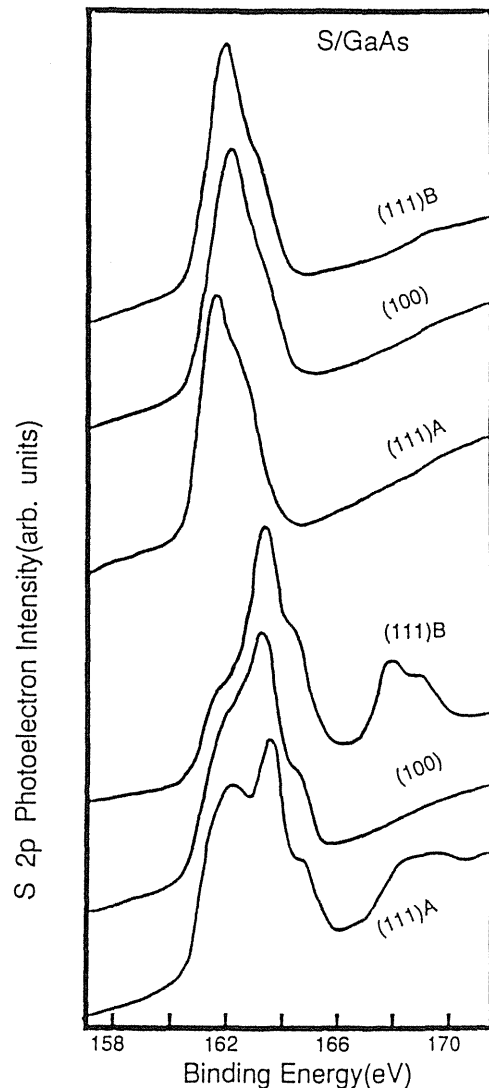


Fig.10 The S 2p spectra are plotted for the (111)A, 100 and (111)B surfaces. The upper three spectra correspond to the S/GaAs substrate annealed at 480 °C for 10 min, while the lower three spectra were measured with no annealing.

annealing, these differences disappear with no remaining As-S bonding and only small spectral differences for the three crystal orientations. In addition, a peak is observed in the high energy region in the 167-170 eV region which is attributed to a SO_x species. This oxide disappears with annealing. To summarize, annealing 1) initiates As-S to Ga-S exchange which passivates the surface, 2) produces a reproducible and well ordered surface and 3) removes surface oxides.

B. Selenium Passivation

In addition to sulfur, selenium has also been shown to be quite effective in passivating the GaAs surface¹⁵⁾⁻¹⁹⁾. Advantages of Se passivation include size compatibility(As and Se radii are nearly identical) and the ability to perform the passivation in UHV. Initially, the Se passivation studies were performed by chemical means and misunderstandings into the mechanism responsible for the Se passivation effect were made¹⁵⁾⁻¹⁸⁾. However, recent in-situ Se passivation studies have clarified the Se passivation mechanism and elucidated both the chemical bonding

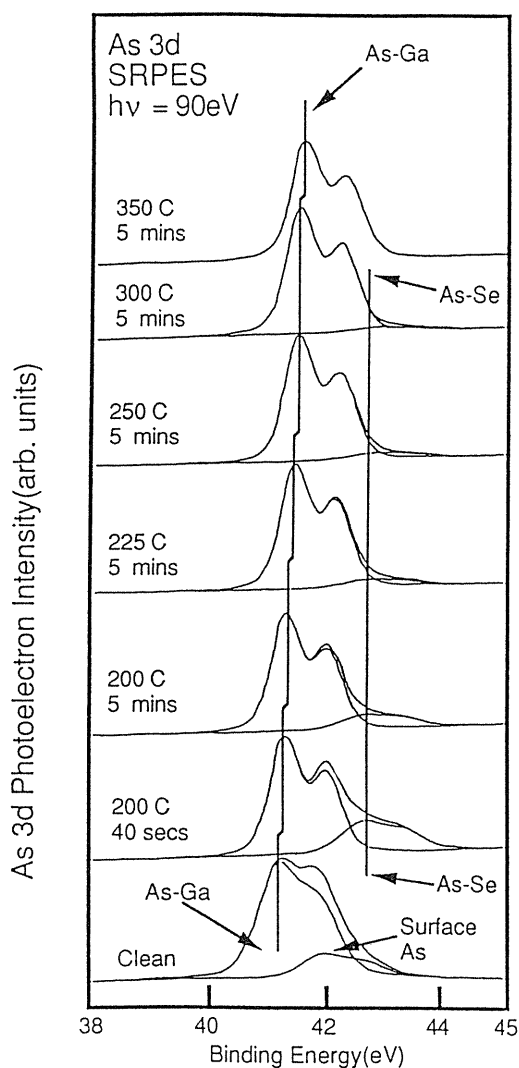


Fig.11 In this figure, the As 3d spectra are plotted as a function of surface treatment. The vertical lines indicate changes in band bending.

and surface structure on the Se/GaAs surface^{20), 62)-67)}. In Fig.11, the As 3d spectra are plotted for a variety of surface treatments. The clean As rich GaAs surface is characterized by an As-Ga and surface As peak, thus yielding a relatively broad As 3d spectrum. One can see from Fig.11 that as the substrate temperature is raised under Se irradiation, the degree of As-Se bonding is reduced and the degree of band bending (higher As 3d peak binding energy shift) also decreases. Details are described elsewhere⁶⁵⁾⁻⁶⁷⁾.

The Se 3d spectrum for Se treated GaAs(100) at a high substrate temperature is shown in Fig.12. In this figure, two spin orbit split Se states separated by about 1 eV are observed after peak deconvolution. Initially, it was believed that the difference in coordination number between surface Se and Se imbedded into the bulk of GaAs near the surface gave rise to these two states⁶⁴⁾⁻⁶⁷⁾. The reasoning was that less charge transfer took place at the Ga-Se bond at

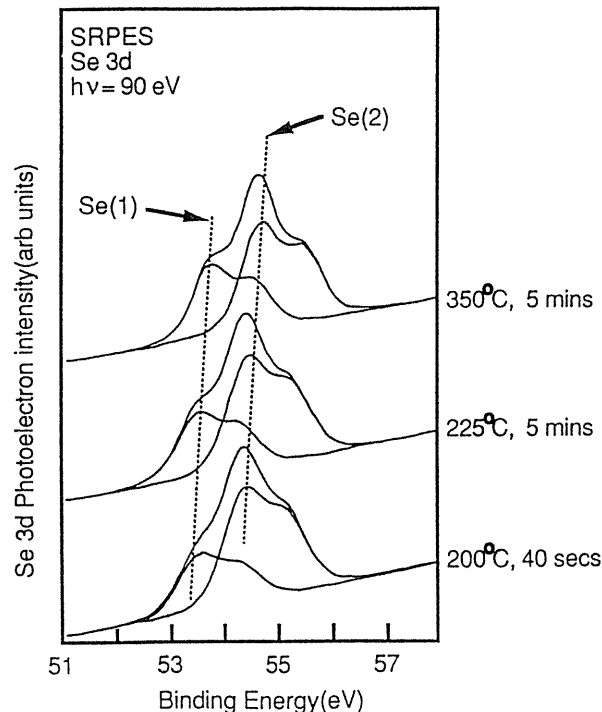


Fig.12 The Se 3d spectrum is plotted for Se deposited on GaAs(100) surface at a high substrate temperature. Peak deconvolution indicates two separate Se states and a Ga vacancy model consistent with these results is shown in the bottom of this figure.

the surface relative to bulk Se giving surface Se a higher binding energy. Recent polar angle resolved measurements by Maeda et al.⁶⁸⁾ indicate that this assignment is incorrect with the low binding energy component ascribed to Se at the GaAs surface. Recently, a number of papers indicate that Ga_2Se_3 can be grown on the GaAs(100) surface with Ga_2Se_3 assuming an $\alpha\text{-Ga}_2\text{Se}_3$ phase structure with Ga vacancies⁶⁹⁻⁷²⁾. EXAFS studies by Takatani et al.⁷³⁾ also indicate that the structure of Se/GaAs is very similar to $\alpha\text{-Ga}_2\text{Se}_3$. A model consistent with the EXAFS and cross sectional TEM results as well as angle resolved SRPES is shown in **Fig.13**⁶⁸⁾. In this case, the Se(1) component has a vacancy as a nearest neighbor, while the high binding energy Se component is bonded to only Ga atoms with no Ga vacancies nearby. A detailed theoretical band or molecular orbital calculation is needed to provide insight into the degree of charge transfer for the two different Se species, but this has not been done yet.

One of the potential advantages of Se is the control of the passivation process since treatment can be done in-situ by MBE. The controllability is demonstrated in **Fig.14**⁷²⁾. In this example, the GaAs substrate was exposed to a Se flux for substrate temperatures ranging from 200 to 350 °C. The results show that the degree of band bending can be controlled by varying the substrate temperature which is correlated also with the degree of As remaining at the surface and degree of Se order. No additional band bending reduction is observed for substrate temperatures exceeding 350 °C, suggesting this is the optimum temperature for Se passivation.

A comparison of S and Se surface passivation based on band bending is made and shown in **Table 1**. One can be from this table that Se provides the opportunity for achieving a nearly flat band condition, which is most likely the result of the greater incorporation of Se in GaAs since the passivation is done at elevated temperatures. In contrast, conventional sulfur passivation is constrained by the limited amount of sulfur that remains on the surface prior to annealing. However, other means of S treatment by atomic $\text{S}^{29)}$, $\text{H}_2\text{S}^{30), 53), 54)}$ and other means³¹⁾⁻³³⁾ may

improve S coverage on the GaAs surface further improving the prospects of passivation. In order to make a complete comparison, other factors such as surface segregation susceptibility, oxidation resistance, epitaxial overgrowth etc. need to be considered as well.

In summary, a number of similar trends are observed for both S and Se passivation. The first is that exposing the GaAs surface to the passivating

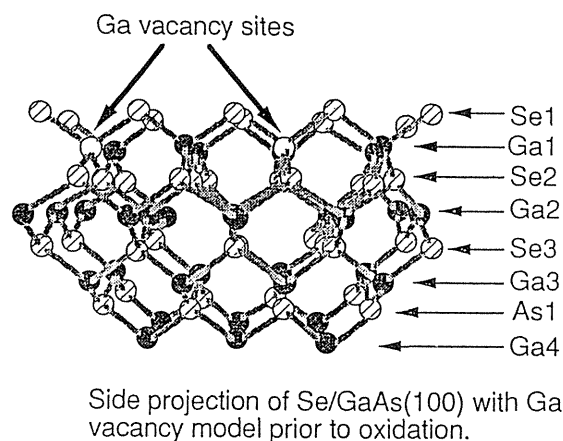


Fig.13 A proposed model for the Se/GaAs(100) surface consistent with the Ga vacancy model.

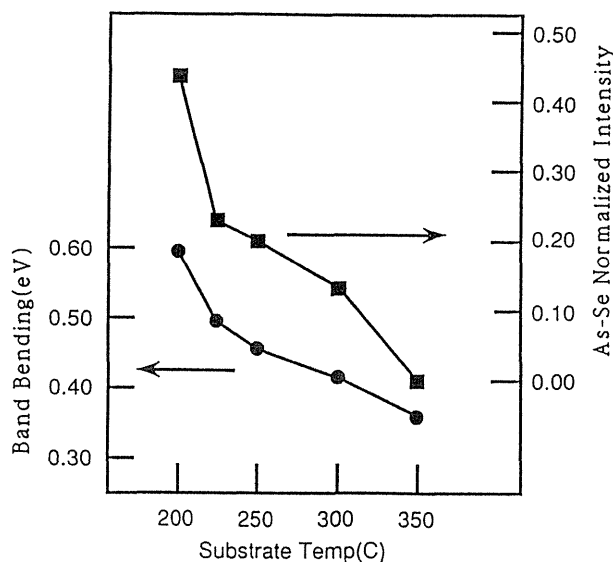


Fig.14 The degree of band bending(left vertical axis) is plotted as a function of substrate temperature. The degree of band bending reduction is also correlated with the degree of remaining As-Se.

Table 1 A concise summary of the band bending changes observed for both S and Se passivation under various conditions.

Sulfur Passivation	Band Bend (eV)	Selenium Passivation	Band Bend (eV)
Clean surface (As rich)	0.8	Clean surface (As rich)	0.8
As-S	0.8	As-Se (RT)	0.6
Ga-S	0.5	250 °C Anneal	0.5
		Ga-Se (550 °C)	0.3
After S Desorption	1.0	After Se Desorption	1.3

agent(S or Se) is not enough to realize passivation and that an activation barrier needs to be surpassed to that surface As is replaced by either S or Se to form the more thermodynamically stable GaS or GaSe species. In the examples here, we have shown that this reaction takes place by simply annealing the GaAs substrate. Others have shown that this reaction can take place by either electron bombardment³²⁾ or exposure to synchrotron radiation³³⁾. The second point to realize that the surface passivation effect is only realized by forming a species that produces less surface states. In the case of Se and S, it is fortuitous that the most thermodynamic state is also the state which produces the fewest surface defect states. Now that the basics of surface passivation have been discussed, the next step is to consider the growth of overlayers and how this effects the passivated surface.

4. Overlayer Deposition

A. CaF₂ Deposition

In order to realize GaAs based devices, an overlayer must be deposited on the passivated surface. The overlayer will of course depend on the nature of the device and application. Let us first consider the deposition of CaF₂ which is an attractive case since the lattice mismatch between CaF₂ and GaAs is small and CaF₂ evaporates as a molecule. An obvious application for depositing an insulator on

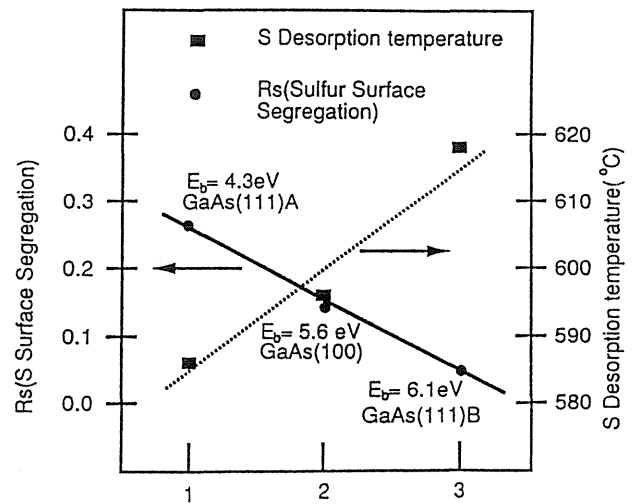


Fig.15 The degree of S surface segregation R_s accompanied by CaF₂ deposition is plotted for the GaAs (111)A, 100 and (111)B surfaces. the figure shows that R_s is correlated with the S desorption temperature, the S-Ga coordination number and the S-Ga theoretical binding energy.

passivated GaAs would be MISFET device. Deposition of CaF₂ on S/GaAs results in surface segregation of S(R_s) which as shown in Fig.15 is directly correlated with the S-Ga coordination number since this varies from 1 to 3 for the (111)A, 100 and (111)B surfaces respectively. The strength of the S-Ga bond is also inferred by the S desorption temperature and theoretical S-Ga binding energy^{55), 74), 75)} which confirms that the S-Ga bond

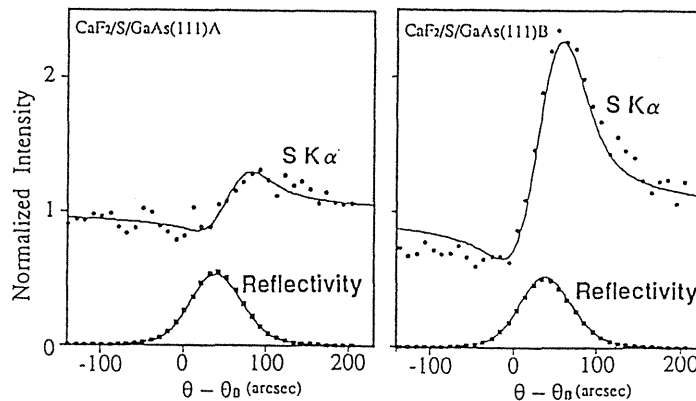
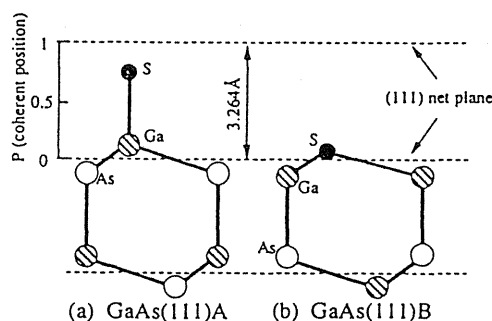


Fig.16 The XSW profile for $\text{CaF}_2/\text{S}/\text{GaAs}(111)\text{B}$ and $(111)\text{A}$.



	(111)A		(111)B	
	S/GaAs	$\text{CaF}_2/\text{S}/\text{GaAs}$	S/GaAs	$\text{CaF}_2/\text{S}/\text{GaAs}$
<i>F</i>	0.59 ± 0.06	0.69 ± 0.04	0.56 ± 0.03	1.0 fixed
<i>P</i>	0.89 ± 0.02	0.80 ± 0.01	0.00 ± 0.02	0.06 ± 0.01

Fig.17 A side view of the $\text{GaAs}(111)\text{A}$ and $(111)\text{B}$ surfaces following CaF_2 deposition, as determined by XSW. The coherent fraction *F* and position *P* are also tabulated in the bottom of the figure for the $(111)\text{A}$ and $(111)\text{B}$ surface prior to and after CaF_2 deposition.

strength is as follows: $(111)\text{B} > 100 > (111)\text{A}$. Thus, the degree to which S remains at the interface in the presence of the CaF_2 overlayer is related to the S-Ga bond strength. These results are also consistent with the x-ray standing wave (XSW) profiles for $\text{CaF}_2/\text{S}/\text{GaAs}(111)\text{A}$ and B obtained by Sugiyama et al.^{74), 75)} and shown in Fig.16. From these profiles, the adsorbate position *P* relative to the (111) net plane can be obtained and is shown in Fig.17. The coherent diffraction parameter *F* indicates the degree of ordering of S with larger values corresponding to greater ordering. The *F* values tabulated in the bottom of

Fig.17 for the two surfaces prior to and after CaF_2 deposition indicates that there is an almost complete ordering for the $(111)\text{B}$ surface, while there is some randomness of the S positions for the $(111)\text{A}$ orientation. Thus, the weak S-Ga bond for the $(111)\text{A}$ surface predisposes S to segregate to the surface and to assume a degree of randomness at the buried interface. In contrast, there is very little S surface segregation and nearly complete S ordering for the stable $\text{CaF}_2/\text{S}/\text{GaAs}(111)\text{B}$ interface. Details of the SRPES and XSW results for this system are discussed in detail elsewhere⁷⁴⁾⁻⁷⁷⁾.

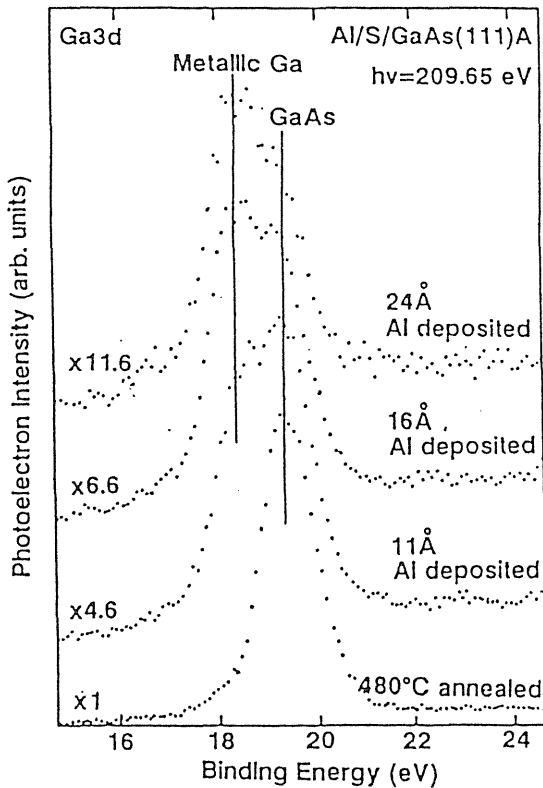


Fig.18 The Ga 3d spectra are plotted for the Al/S/GaAs(111)A surface for various Al overlayer thicknesses. Note that Al deposition results in the formation of metallic Ga.

B. Al/S/GaAs

The Al/S/GaAs interface is another interesting interface example. In this case, deposition of Al on S passivated GaAs is characterized by an Al to Ga exchange reaction in the photoelectron spectra shown in Fig.18. To further investigate this system, depth profiling via sputter Auger Electron Spectroscopy(AES) was performed on a similar sample(Al/S/GaAs(111)A), as shown in Fig.19. In this depth profile, segregation of Ga to the surface is observed while S remains at the Al/S/GaAs interface. These results are consistent with the relative thermodynamic strength of Al-S relative to either Al-Ga or Ga-S⁵⁶. The position of the S atom at the Al/S/GaAs interface was also investigated by Sugiyama et al.⁷⁸ using XSW with the experimental data and theoretical fits plotted in Fig.20. One can see that as a result of the exchange reaction, the S atoms become more disordered upon Al deposition and that disorder is greater at the relatively unstable (111)A interface. The Schottky Barrier Heights(SBH) are also shown in Table 2 where the SBH value approaches the ideal Schottky barrier limit, but is still far from the theoretical limit. Several reasons for this include incomplete passivation and damage during Al deposition.

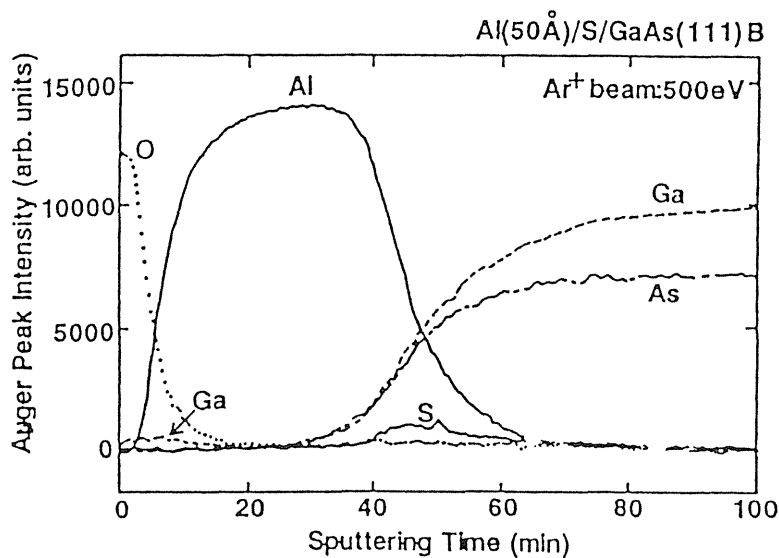


Fig.19 An Auger sputtering depth profile for the Al/S/GaAs(111)A which indicates formation and surface segregation of metallic Ga with Al deposition, while S remains at the buried interface.

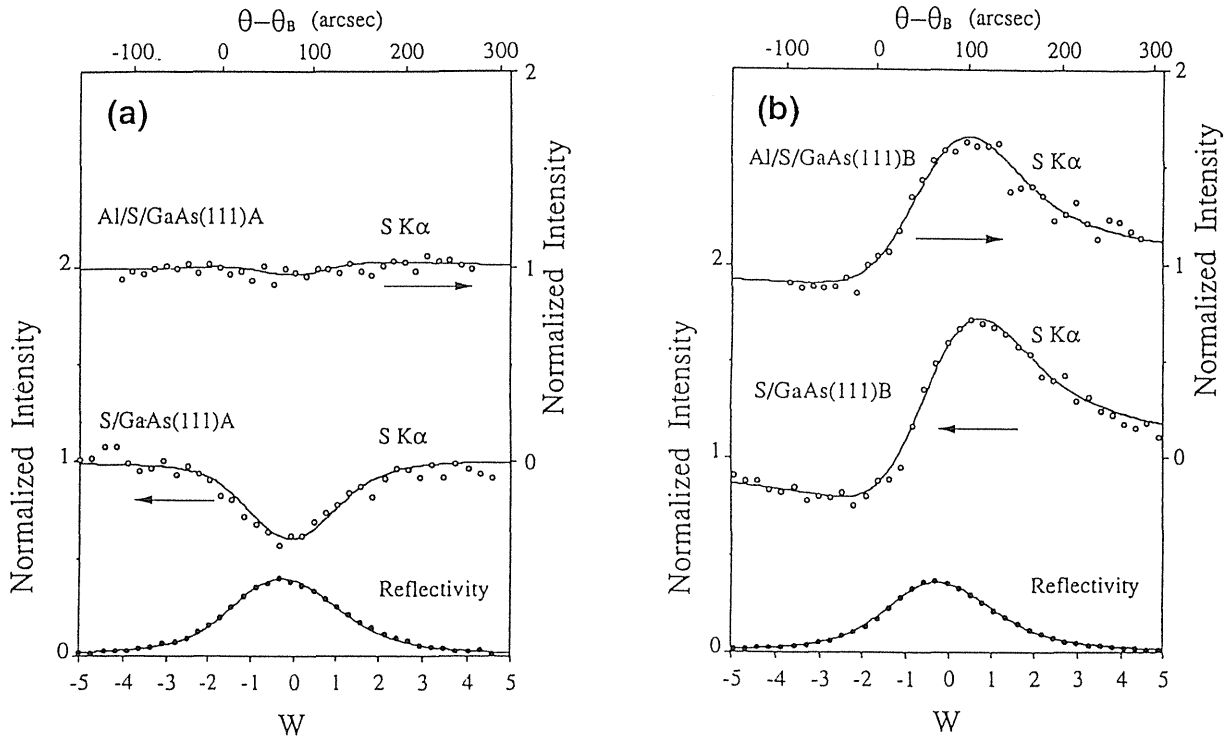


Fig.20 The XSW profiles are shown for both Al/S/GaAs(111)A and Al/S/GaAs(111)B.

5. Problems and Proposed Solutions

A. Surface Segregation and Intermixing

In this section, two problems that have limited the development of this field will be addressed: surface segregation and oxidation. The deposition of Pd on the S/GaAs surface illustrates the problem of surface segregation upon overlayer deposition since Pd is a fairly reactive metal and is well known to react with both As and Ga. The work is also motivated in part by the high work function of Pd which should in theory result in a diode with a high SBH. Until now, this has not been realized since surface defect states pin the Fermi level resulting in a much lower SBH. The XSW profiles for Pd/S/GaAs(111)A and B are plotted in Fig.21⁷⁵⁾. The similarity in the reflectivity and XSW profiles for both the (111)A and (111)B surfaces indicate that the S atoms are relatively randomly distributed with respect to the (111) crystal planes. SRPES measurements indicate that Pd reacts with As and Ga and also causes S to segregate to the surface⁷⁹⁾. This is confirmed by the Auger sputtering depth profile shown in Fig.22. As one can see in this

Table 2 The electrical characteristics are shown for the Al/S/GaAs(111)A and Al/S/GaAs(111)B systems.

Electrical Characteristics

Metal/GaAs: Schottky Diode (I-V)

I. Al deposition:

Sample	(111) A	(111) B
Al/S/GaAs	0.62 eV	0.57 eV
Al/GaAs	0.7-8 eV	0.66 eV

Ideal value: 0.21 eV

Al/S/GaAs closer to ideal SBH than Al/GaAs

Passivation effect, but not complete:

1. Incomplete passivation, coverage etc.
2. Gap states induced by metal, exchange etc.

figure, S segregates to the surface with no S remaining at the Pd/GaAs interface. I-V characteristics were also performed and the results compiled

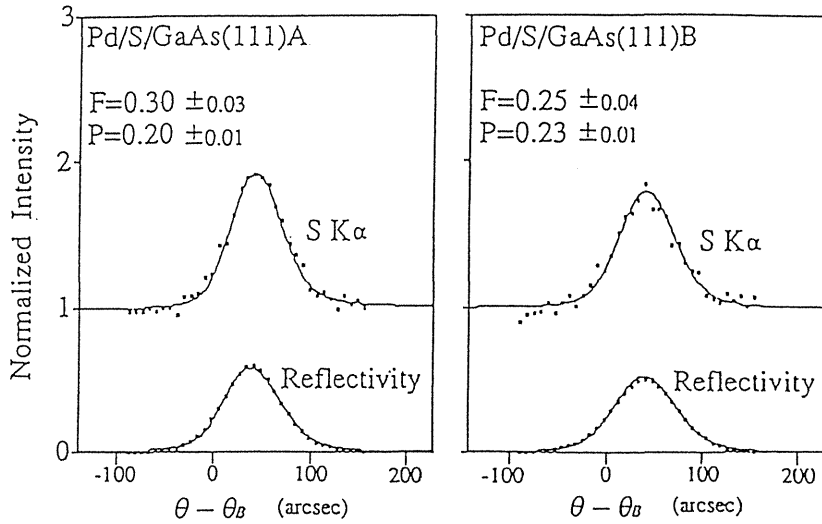


Fig.21 The XSW profiles are shown for both Pd/S/GaAs(111)A and Pd/S/GaAs(111)B. The similarity between the XSW profiles and the reflectivity yields indicates that S is randomly distributed with respect to the (111) crystal planes.

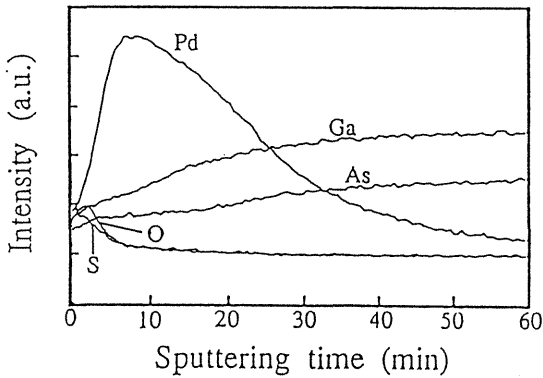


Fig.22 An Auger depth profile was performed. In contrast to Al/S/GaAs, all of the sulfur segregates to the surface. These measurements are consistent with SRPES measurements where Pd causes S segregation and forms compounds with As and Ga resulting in a degradation of the interface.

in **Table 3**. In this table, one can see that while there is a difference between the SBH for the (111)A and (111)B surfaces(which is not understood at this time), there is no difference between the Pd/S/GaAs and Pd/GaAs systems. This is expected since no S remains at the surface following Pd deposition. Recent attempts to mitigate this surface segregation and alloying has been attempted with some success

Table 3 The electrical characteristics are shown for the Pd/S/GaAs(111)A and Pd/S/GaAs(111)B systems.

II. Pd deposition:

Sample	(111) A	(111) B
Pd/S/GaAs	0.79 eV	0.89 V
Pd/GaAs	0.79 eV	0.89 V

Ideal value: 1.05 eV

Reactions at interface, passivation effect destroyed

Pd/S/GaAs and Pd/S/GaAs pinned at same level

by depositing a stable buffer layer between S and Pd⁸⁰⁾.

Another promising buffer layer candidate is Ga₂Se₃, since this material can be grown on a GaAs substrate^{70)-72), 81)}. The graphite like nature of Ga₂Se₃ not only relaxes the lattice mismatching of heteroepitaxial growth, but also seems to mitigate damage induced by overlayer deposition, as indicated by the ideal Schottky Barrier Heights obtained for a variety of metals deposited on a Ga₂Se₃ substrate^{82), 83)}.

B. Oxidation

One of the major problems with GaAs surface passivation is that the surface is quickly degraded and the full effects of passivation lost upon exposing the passivated sample in air. In order to understand the mechanism in which this degradation takes place, oxidation studies have been performed both on the S and Se passivated GaAs surface⁸⁴. In Fig.23, the PL intensity is plotted for the S/GaAs passivated surface as a function of exposure time in atmosphere. The figure clearly shows that the effects of surface passivation are completely lost after only 10 minutes of exposure. To insure that the degradation was not artificially induced by the laser source, similar time dependent PL measurements ("in vacuum") were performed. The results unequivocally demonstrate that degradation is a result of surface degradation from exposure in atmosphere.

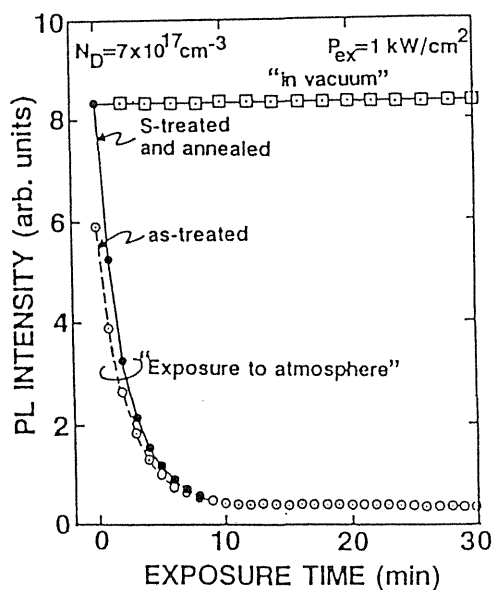


Fig.23 The PL intensity is recorded for a sulfur passivated GaAs(100) sample as a function of exposure time in atmosphere. The results indicate the PL intensity degrades within a short time(10 minutes) as a result of oxidation that generates surface defect states. The "in-vacuum" measurements were performed to insure that the PL intensity reduction was not caused by any laser induced artifacts during the PL measurements.

In order to correlate the PL measurements with surface chemical bonding changes, SRPES measurements were also performed. The Ga 3d spectra shown in Fig.24 indicates that this degradation is associated with surface oxidation. The details of surface oxidation are similar for S and Se passivation and proceeds with Ga first being oxidized, followed by As and S(or Se). Band bending changes are observed before many of the chemical bonding changes are observed indicating that only a small degree of surface degradation gives rise to a significant increase in surface defect states seriously degrading the passivated surface. Details of the surface oxidation mechanism are discussed in detail elsewhere^{84), 85)}

A possible way of overcoming the deleterious effects of surface oxidation is to deposit an overlayer which can react with oxygen and induce oxygen to segregate to the overlayer. Suitable overlayers can be considered on the basis of the relative stability of the overlayer oxide relative to any possible substrate oxides(Ga_2O_3 is the most stable oxide component for GaAs the oxidized S/GaAs system). A suitable candidate is Al since the Heat of Formation, a good indicator for thermodynamic stability, for Al_2O_3 is much greater than Ga_2O_3 . In order to demonstrate this idea, a Se passivated GaAs(100) sample was exposed for one hour in atmosphere. After exposure,

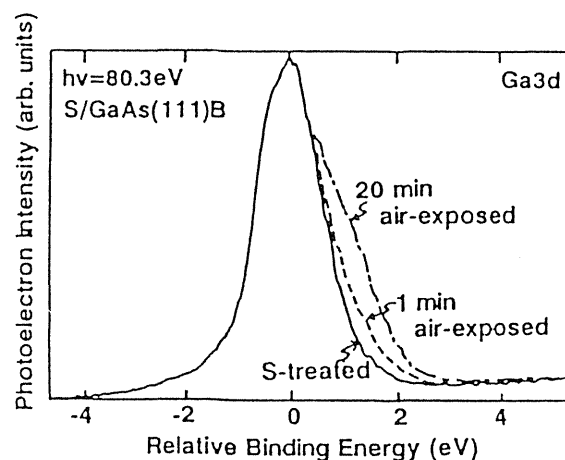


Fig.24 The Ga 3d SRPES spectra were recorded as a function of atmospheric exposure time indicating that PL degradation is indeed associated with surface oxidation.

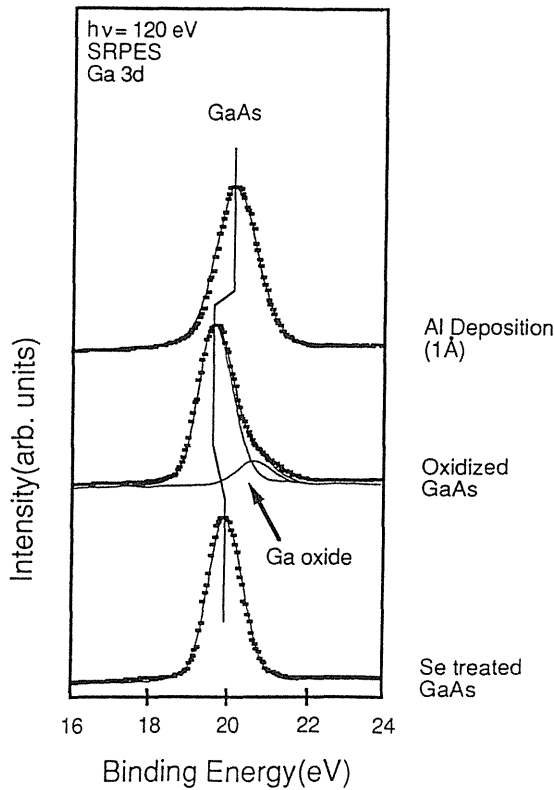


Fig.25 Deposition of a very thin Al overlayer on the oxidized (and degraded) Se/GaAs surface rejuvenates the surface since the oxygen segregates and combines with the Al overlayer.

a high binding energy component attributed to Ga_2O_3 was observed and a low B. E. Shift ascribed to a band bending increase was observed. Following exposure, the sample was placed in the vacuum chamber where a very thin Al overlayer was deposited. The Ga 3d spectra for this case is shown in the top of Fig.25. Curve fitting has been performed and indicates a good fit between the raw data and the synthetic spectra. Further, no Ga oxide component was observed. Finally, a significant band bending reduction was observed resulting in a flatter band relative to the unoxidized Se/GaAs surface. Thus, this study indicates that the degraded surface can be rejuvenated by deposition of an appropriate overlayer. The overlayer oxide is expected to be stable and thus may also prevent or at least mitigate surface segregation of S or Se accompanying desorption of a reactive overlayer such as Pd. Details of this work are discussed elsewhere⁸⁶⁾.

In addition, recent investigations using As_2S_3 as a capping layer have been attempted since this impermeable glassy compound prevents oxygen from diffusing to the GaAs surface. Recent studies have indicated that the passivation effect can last as long as 4 months^{87), 88)}.

6. Conclusions

The surface chemical bonding and structure of the S and Se passivated GaAs surface have been investigated in detail by SRPES. The XSW technique also provides unique information on S at the buried interface in a nondestructive manner. The results indicate that to realize the full effect of surface passivation, an As to S(Se) exchange is necessary, thus requiring thermal annealing. Thermal annealing also results in the removal of surface oxides and a more reproducible surface for S treated GaAs. The passivation of GaAs by Se has also been demonstrated indicating the superior control achieved by this technique since passivation can be done in UHV. In addition, a Ga vacancy model for the Se/GaAs surface is proposed. The key point seems to be in overcoming an activation barrier so that S or Se can replace As located at the surface to form a more thermodynamically stable GaS(Se) species that also reduces the number of surface defect states.

The deposition of overlayers on the S passivated GaAs surface by three different overlayers illustrate the different types of phenomena that can be observed in these interfacial studies. Deposition of CaF_2 on S/GaAs results in S surface segregation that is correlated with the S-Ga bond strength. In addition, the degree of sulfur ordering at the $\text{CaF}_2/\text{S}/\text{GaAs}$ interface is greater for the (111)B surface where S segregation is very small. Deposition of Al on S/GaAs results in Al to Ga exchange, surface segregation of metallic Ga and the formation of a thermodynamically stable Aluminum Sulfide interlayer. Deposition of Pd results in complete segregation of S to the surface and complete destruction of the passivation effect.

Finally two problems associated with surface passivation, surface segregation and oxidation, were

discussed and possible solutions to these problems explored. An innovative method for rejuvenating the oxidized passivated surfaces was also demonstrated that results in a surface with little band bending and a stable interface that may also prevent S(or Se) segregation upon deposition of a reactive overlayer such as Pd.

7. Acknowledgements

This review is a summary of the work performed by us and the following people: M. sugiyama(NTT), F. Maeda(NTT), Y. Muramatsu(NTT), H. Sugahara(NTT), Y. Watanabe(NTT), S. Maeyama(NTT), H. Oigawa(Tsukuba University), R. Berrigan and H. Hashizume(Tokyo Institute of Technology). We are also indebted to M. Sugiyama, F. Maeda, Y. Watanabe, S. Maeyama, H. Oigawa and R. Berrigan for useful discussions.

References

- 1) J. Massies, F. Dezaly and N. T. Linh, *J. Vac. Sci. Technol.* **17**, 1134 (1980).
- 2) C. J. Sandroff, R. N. Nottenburg, J. -C. Bischoff and R. Bhat, *Appl. Phys. Lett.* **51**, 33 (1987).
- 3) M. S. Carpenter, M. R. Melloch and T. E. Dugan, *Appl. Phys. Lett.* **53**, 66 (1988).
- 4) K. C. Hwang and S. S. Li, *J. Appl. Phys.* **67**, 2162 (1990).
- 5) H. Oigawa, J. Fan, Y. Nannichi, H. Sugahara and M. Oshima, *Jpn. J. Appl. Phys.* **30**, L322 (1991).
- 6) J. Fan, H. Oigawa and Y. Nannichi, *Jap. J. Appl. Phys.* **27**, L1331 (1988).
- 7) J. Fan, Y. Kurata and Y. Nannichi, *Jap. J. Appl. Phys.* **28**, L2255 (1989).
- 8) H. Ricard, K. Aizawa and H. Ishiwara, *Appl. Surf. Sci.* (1991).
- 9) H. Ricard, K. H. Kim, K. Aizawa and H. Ishwara, *Jap. J. Appl. Phys.* **29**, L2460 (1990).
- 10) H. H. Lee, R. J. Racicot and S. H. Lee, *Appl. Phys. Lett.* **54**, 724 (1989).
- 11) R. S. Besser and C. R. Helms, *J. Appl. Phys.* **65**, 4306 (1989).
- 12) S. Shikata and H. Hayashi, *J. Appl. Phys.* **70**, 3721 (1991).
- 13) D. Liu, T. Zhang, R. A. LaRue, J. S. Harris, Jr. and T. W. Sigmon, *Appl. Phys. Lett.* **53**, 1059 (1988).
- 14) D. E. Aspens, *Surf. Sci.* **132**, 406 (1983).
- 15) C. J. Sandroff, M. S. Hegde, L.A. Farrow, R. Bhat, J. P. Harbison and C. C. Chang, *J. Appl. Phys.* **67**, 586 (1990).
- 16) F. S. Turco, C. J. Sandroff, D. M. Hwang, T. S. Ravi, and M. C. Tamargo, *J. Appl. Phys.* **68**, 1038 (1990).
- 17) F. S. Turco, C. J. Sandroff, M. S. Hegde and M. C. Tamargo, *J. Appl. Phys.* **B8**, 856 (1990).
- 18) C. J. Sandroff, F.S. Turco-Sandroff, L. T. Florez and J. P. Harbison, *J. Appl. Phys.* **70**, 3632 (1991).
- 19) S. Takatani and M. Nakazawa, In *Modification of GaAs(100) Surface by Se and Formation of Amorphous-Se/GaAs(100) Heterostructure*, Proceedings of the International Symposium on GaAs and Related Compounds, edited by K. E. Singer, IOP Conf. Proc. No. 112 (Institute of Physics, Bristol, 1990), Chap. 3, p.111.
- 20) Y. Tao, A. Yelon, E. Sacher, Z. H. Lu and M. J. Graham, *Appl. Phys. Lett.* **60**, 2669 (1992).
- 21) A. Nelson, S. Frigo and R. Rosenberg, *J. Appl. Phys.* **71**, 6086 (1992).
- 22) M. Faur, M. Faur, P. Jenkins, M. Goradia, S. GBailey, D. Jayne, I. Weinberg and C. Goradia, *Surf. and Interfacial Anal.* **15**, 745 (1990).
- 23) C. W. Wilmsen, K. M. Geib, J. Shin, R. Iyer, D. L. Lile and J. Pouch, *J. Vac. Sic. Technol.* **B7**, 851 (1989).
- 24) R. Iyer, R. R. Chang and D. L. Lile, *Appl. Phys. Lett.* **53**, 134 (1988).
- 25) R. Iyer and D. L. Lile, *Appl. Phys. Lett.* **59**, 437 (1991).
- 26) G. Hollinger, R. Blanchet, M. Gendry, C. Santinelli, R. Skheyta and P. Viktorovitch, *J. Appl. Phys.* **67**, 4173 (1990).
- 27) Y. Fukuda, N. Sanada, M. Kuroda and Y. Suzuki, *Appl. Phys. Lett.* **61**, 955 (1992).
- 28) H. Oigawa, J. F. Fan, Y. Nannichi, H. Sugahara and M. Oshima, *Jpn. J. Appl. Phys.* **30**, L322 (1991).
- 29) G. Y. Gu, E. A. Ogryzlo, P. C. Wong, M. Y. Zhou and KA. R. Mitchell, *J. Appl. Phys.* **72**, 762 (1992).
- 30) T. Tiedje, K. M. Colbow, D. Rogers, Z. Fu and W.

- Eberhardt, *J. Vac. Sci. Technol.* **B7**, 837 (1989).
- 31) X. Y. Hou, Z. S. Li, W. Z. Cai, X. M. Ding and X. Wang, Extended Abstracts of the 1992 International Conference on Solid State Devices and Materials, Tsukuba, 1992, (The Japan Society of Physics) pp.272-274.
- 32) Y. C. Du, H. Wang, D. C. Sun and F. M. Li, Extended Abstracts of the 1992 International Conference on Solid State Devices and Materials, Tsukuba, 1992, (The Japan Society of Physics) pp.260-262.
- 33) Y. Takakuwa, M. Niwano, S. Fujita, Y. Takeda and N. Miyamoto, *Appl. Phys. Lett.* **58**, 1635 (1991).
- 34) H. L. Chuang, M. S. Carpenter, M. R. Melloch, M. S. Lundstrom, E. Yablonovitch and T. J. Gmitter, *Appl. Phys. Lett.* **57**, 2113 (1990).
- 35) S. Shikata, H. Okada and H. Hayashi, *J. Appl. Phys.* **69**, 2717 (1991).
- 36) M. S. Carpenter, M. R. Melloch, M. S. Lundstrom and S. P. Tobin, *Appl. Phys. Lett.* **52**, 2157 (1988).
- 37) H. Kawanishi, H. Ohno, T. Morimoto, S. Kaneiwa, N. Miyaguchi, H. Hayashi, Y. Akagi, Y. Nakajima and T. Hijikata, Extended Abstracts of the 21st Conference on Solid State Devices and Materials, Tokyo, 1989, (The Japan Society of Physics) pp.337-340.
- 38) M. G. Mauk, S. Xu, D. J. Arent, R. P. Mettens and G. Borghs, *Appl. Phys. Lett.* **54**, 213 (1989).
- 39) D. Wong, J. E. Schlesinger and A. G. Milnes, *IEEE Electronic Device Lett.* **11**, 321 (1990).
- 40) M. Oshima, T. Kawamura, S. Maeyama and T. Miyahara, *J. Vac. Sci. Technol.* **A6**, 1451 (1988).
- 41) T. Kawamura, S. Maeyama, M. Oshima, Y. Ishi and T. Miyahara, *Rev. Sci. Instrum.* **60**, 1928 (1989).
- 42) S. Maeyama et al., To be published in *Rev. Sci. Instrum.*
- 43) For example, see B. N. Dev, V. Aristov, N. Hertel, T. Thundat and W. M. Gibson, *Surf. Science* **163**, 457 (1985).
- 44) Y. Nannichi, J. Fan, H. Oigawa and A. Koma, *Jap. J. Appl. Phys.* **27**, 2367 (1988).
- 45) C. J. Sandroff, M. S. Hegde, L. A. Fallow, C. C. Chang and J. P. Harbison, *Appl. Phys. Lett.* **54**, 362 (1989).
- 46) B. A. Cowans, Z. Dardas, W. N. Delgass, M. S. Carpenter and M. R. Melloch, *Appl. Phys. Lett.* **54**, 365 (1989).
- 47) C. J. Sandroff, M. S. Hegde and C. C. Chang, *J. Vac. Sci. Technol.* **B7**, 841 (1989).
- 48) M. S. Carpenter, M. R. Melloch, B. A. Cowans, Z. Dardas and W. N. Delgass, *J. Vac. Sci. Technol.* **B7**, 845 (1989).
- 49) C. J. Spindt, R. S. Besser, R. Cao, K. Miyano, C. R. Helms and W. E. Spicer, *Appl. Phys. Lett.* **54**, 1148 (1989).
- 50) C. J. Spindt, D. Liu, K. Miyano, P. L. Meissner, T. T. Chiang, T. Kendelewicz, I. Lindau and W. E. Spicer, *Appl. Phys. Lett.* **55**, 860 (1989).
- 51) K. M. Geib, J. Shin and C. W. Wilmsen, *J. Vac. Sci. Technol.* **B8**, 838 (1990).
- 52) J. Shin, K. M. Geib, C. W. Wilmsen and Z. Lillenthal-Weber, *J. Vac. Sci. Technol.* **A8**, 1984 (1990).
- 53) H. Sugahara, M. Oshima, H. Oigawa, H. Shigekawa and Y. Nannichi, *J. Appl. Phys.* **69**, 4349 (1991).
- 54) H. Sugahara, M. Oshima, R. Klausner, H. Oigawa and Y. Nannichi, *Surf. Science* **242**, 335 (1991).
- 55) T. Scimeca, Y. Muramatsu, M. Oshima, H. Oigawa and Y. Nannichi, *Phys. Rev. B* **44**, 12927 (1991).
- 56) O. Kubaschewski et al., in *Metallurgical Thermochemistry*, 5th ed. (Pergamon, New York, 1979).
- 57) H. Oigawa, unpublished results.
- 58) T. Ohno and K. Shiraishi, *Phys. Rev.* **B42**, 11194 (1990).
- 59) T. Ohno, *Phys. Rev.* **B44**, 6306 (1991).
- 60) W. E. Spicer, I. Lindau, P. Skeath and C. Y. Su, *J. Vac. Sci. Technol.* **17**, 1019 (1980).
- 61) H. Hasegawa and H. Ohno, *J. Vac. Sci. Technol.* **B4f**, 1130 (1986).
- 62) S. A. Chambers and V. S. Sundaram, *Appl. Phys. Lett.* **57**, 2342 (1990).
- 63) S. A. Chambers and V. S. Sundaram, *J. Vac. Sci. Technol.* **B9**, 2256 (1991).
- 64) S. Takatani, T. Kikawa and M. Nakazawa, *Phys. Rev.* **B45**, 8498 (1992).
- 65) T. Scimeca, Y. Watanabe, R. A. Berrigan and M. Oshima, *Phys. Rev.* **B46**, 10201 (1992).
- 66) T. Scimeca, Y. Watanabe, R. Berrigan and M. Oshima, 1992 (SSDM) Proceedings.
- 67) T. Scimeca, Y. Watanabe and M. Oshima, To appear in *Appl. Phys. Lett.*
- 68) F. Maeda, Y. Watanabe, T. Scimeca and M. Oshima, To be published in *Phys. Rev. B*.

- 69) D. Li, Y. Nakamura, N. Otsuka, J. Qiu, M. Kobayashi and R. L. Gunshor, *Surf. Science* **267**, 181 (1992).
- 70) D. Li, Y. Nakamura, N. Otsuka, J. Qiu, M. Kobayashi and R. L. Gunshor, *J. Crystal Growth* **111**, 1038 (1991).
- 71) D. Li, Y. Nakamura, N. Otsuka, J. Qiu, M. Kobayashi and R. L. Gunshor, *J. Vac. Sci. Technol.* **B9**, 2167 (1991).
- 72) J. Qiu, M. Kobayashi and R. L. Gunshor, D. Li, Y. Nakamura, N. Otsuka, *Appl. Phys. Lett.* **58**, 2788 (1991).
- 73) S. Takatani, A. Nakano, K. Ogata and T. Kikawa *Jpn. J. Appl. Phys.* **31**, L458 (1992).
- 74) M. Sugiyama, S. Maeyama, M. Oshima, H. Oigawa, Y. Nannichi and H. Hashizume, *Appl. Phys. Lett.* **60**, 3247 (1992).
- 75) M. Sugiyama, S. Maeyama, T. Scimeca, M. Oshima, Y. Watanabe, H. Oigawa and Y. Nannichi and H. Hashizume, 1992 (SSDM) Proceedings.
- 76) T. Scimeca, Y. Muramatsu, M. Oshima, H. Oigawa and Y. Nannichi *Journal of Applied Physics*, **71**, 4405 (1992).
- 77) T. Scimeca, Y. Muramatsu, M. Oshima, H. Oigawa and Y. Nannichi, *Appl. Surf. Sci.*, **60/61**, 256 (1992).
- 78) M. Sugiyama, S. Maeyama and M. Oshima, submitted to *Appl. Phys. Lett.*
- 79) R. A. Berrigan, Y. Watanabe, T. Scimeca and M. Oshima, *Japanese Journal of Applied Physics*, **31**, 3523 (1992).
- 80) M. Oshima, H. Oigawa, T. Scimeca and Y. Nannichi, unpublished results.
- 81) K. Ueno, H. Abe, K. Saiki and A. Koma, *Jpn. J. Appl. Phys.* **30**, L1352 (1991).
- 82) G. J. Hughes, A. McKinley, R. H. Williams and I. T. McGovern, *J. Phys. C: Solid State Phys.*, **15**, L159 (1982).
- 83) I. T. McGovern, J. F. McGilp, G. J. Hughes, A. McKinley, R. H. Williams and D. Norman, *Vacuum*, **33**, 607 (1983).
- 84) M. Oshima, T. Scimeca, Y. Watanabe, H. Oigawa and Y. Nannichi, To appear in *Jpn. J. Appl. Phys.*
- 85) T. Scimeca, R. A. Berrigan, Y. Watanabe and M. Oshima, To appear in *J. Vac. Sci. Technol.*
- 86) T. Scimeca, Y. Watanabe, F. Maeda and M. Oshima, Submitted to *Appl. Phys. Lett.*
- 87) H. L. Chuang, M. S. Carpenter, M. R. Melloch, M. S. Lundstrom, E. Yablonovitch and T. J. Gmitter, *Appl. Phys. Lett.* **57**, 2113 (1990).
- 88) Y. Maeda, K. Wada and Y. Wada, *Appl. Phys. Lett.* **61**, 2993 (1992).

